Photogrammetric Record, 23(121): 6–18 (March 2008)

A CONVERGENT IMAGE CONFIGURATION FOR DEM EXTRACTION THAT MINIMISES THE SYSTEMATIC EFFECTS CAUSED BY AN INACCURATE LENS MODEL

RENE WACKROW (r.wackrow@lboro.ac.uk),
JIM H. CHANDLER (j.h.chandler@lboro.ac.uk),
Loughborough University

(Based on a contribution to the Annual Conference of the Remote Sensing and Photogrammetry Society at Newcastle, 12th September 2007)

Abstract

The internal geometry of consumer grade digital cameras is generally considered unstable. Research conducted recently at Loughborough University indicated the potential of these sensors to maintain their internal geometry. It also identified residual systematic error surfaces or "domes", discernible in digital elevation models (DEMs) (Wackrow et al., 2007), caused by slightly inaccurate estimated lens distortion parameters. This paper investigates these systematic error surfaces and establishes a methodology to minimise them. Initially, simulated data were used to ascertain the effect of changing the interior orientation parameters on extracted DEMs, specifically the lens model. Presented results demonstrate the relationship between "domes" and inaccurately specified lens distortion parameters. The stereopair remains important for data extraction in photogrammetry, often using automated DEM extraction software. The photogrammetric normal case is widely used, in which the camera base is parallel to the object plane and the optical axes of the cameras intersect the object plane orthogonally. During simulation, the error surfaces derived from extracted DEMs using the normal case, were compared with error surfaces created using a mildly convergent geometry. In contrast to the normal case, the optical camera axes intersect the object plane at the same point. Results of the simulation process clearly demonstrate that a mildly convergent camera configuration eradicates the systematic error surfaces. This result was confirmed through practical tests and demonstrates that mildly convergent imagery effectively improves the accuracies of DEMs derived with this class of sensor.

KEYWORDS: camera calibration, convergent image configuration, digital camera, close range photogrammetry

INTRODUCTION

Accurate spatial measurement remains an enduring quest in photogrammetry, which is especially important since consumer grade digital cameras are increasingly used. Convenience, portability and low cost are main advantages and their potential to maintain their temporal stability and manufacturing consistency was demonstrated in Wackrow et al. (2007). However, this work also identified residual systematic error surfaces or "domes", discernible in digital elevation models (DEMs) of difference.

The purpose of this paper is to assess the relationship between these "domes" and an inaccurately specified lens model, as well as to investigate the potential of a mildly convergent image configuration to minimise the systematic error surfaces in DEMs. Previous work related to image configuration is reviewed, before describing the methodology developed to minimise the systematic error surfaces. The relationship between error surfaces, lens model and image configuration is introduced; followed by simulated and experimental results. Finally, this paper concludes with discussion and a brief summary.

PREVIOUS WORK ON IMAGE CONFIGURATION

Appropriate network configurations for camera calibration through self-calibration have been well described in many publications (Fraser, 2006; Remondino and Fraser, 2006). Gruen and Beyer (2001) investigated the determinability of self-calibration parameters under various network conditions (one frame up to eight frames). Of all configurations tested in this study, only an eight frame configuration (convergent, large horizontal base plus vertical base plus additional 90 degrees rotation of frames) produced very good results. This work also indicated that of all interior orientation parameters, the radial distortion is the major source of image deformation.

Karara and Aziz (1974) investigated accuracies in object-space coordinates for four non-metric cameras and a metric camera using the Direct Linear Transformation. Image pairs were taken with each of the cameras with the camera axis approximately horizontal and convergence of about 30 degrees. Somewhat surprisingly, Karara and Aziz (1974) stated that a strong association between increasing the convergence angle of an image pair and improving precision was not found. The authors concluded that the most desirable configuration is the normal case. Should the normal case not be feasible, the angle of convergence should be kept as small as possible. This result is contrary to the finding described in this paper.

The use of mildly convergent image configurations for DEM generation is less frequently reported in literature. The reason might be that the photogrammetric normal case is widely used in automated DEM extraction software. However, an approach using a convergent stereo pair for modelling tooth replicas was reported in the field of medical science (Grenness et al., 2005). A semi-metric camera was used to capture multiple convergent images (5, 10, 15, 20 and 25 degrees) of a planar array and used for camera calibration. The estimated camera parameters and digitised images of tooth replicas were imported

into a commercial digital photogrammetric software package and DEMs were generated. However, the results are unclear and suggest no association between increasing the convergence angle of the image pairs and increasing precision.

This review of previous work identified some uncertainties, suggesting the need for further investigation in the use of convergent imagery for DEM extraction.

THE RELATIONSHIP BETWEEN "DOMES" AND IMAGE CONFIGURATION

Residual systematic error surfaces or "domes" discernible in DEMs of difference were identified in past research conducted by the authors. Metric capabilities of low-cost digital sensors were investigated in Chandler et al. (2005), whilst the geometric stability and consistency of seven identical consumer grade digital cameras was demonstrated in Wackrow et al. (2007). More recently, research identified a significant dependency between these systematic error surfaces, the lens model and image configuration through the use of simulation.

The simulation process

A variety of parameters have to be determined when using a digital camera for accurate photogrammetric measurement, normally derived using self-calibration methods (Fryer, 2001). It was recognised that these parameters needed to be controlled in order to improve understanding, but the variability and uncertainties caused by conducting practical work prevented this. The use of simulated data was considered to be an alternative and more productive approach.

A virtual test field (1·4×1·3m) was conceived, composed of evenly distributed *XYZ* coordinates of hundreds of points. These coordinates were used to create a DEM at 1 mm resolution known as the "Truth DEM". A simulation approach (Fryer et al., 1994) was used to compute perfect photo coordinates from the *XYZ* coordinates of each point of the virtual test field; using predefined interior and exterior orientation. Interior orientation parameters representing a Kodak DCS 460 digital camera were used to provide representative camera information including: principal distance, principal point offset and one parameter (k_1) to model the radial distortion. A vertical stereo image pair was selected, in which each image covered the whole of the test field at a camera to object distance set to 2·5m, and a base-to-distance ratio of 1:7. The geometry of this pair was described by two sets of exterior orientation parameters. The derived photo coordinates and the interior and exterior orientation parameters were then re-established using an external bundle adjustment GAP (Chandler and Clarke, 1992) to compute object coordinates for each point. This provided the opportunity to control each parameter set, representing the interior and exterior orientation, independently. The impact of changing one of these parameters was therefore reflected by the computed object coordinates, which are normally of paramount importance to users. The 3D surfacing tool of the ERDAS IMAGINE 8.7 software was employed to create a DEM through interpolation at 3 mm resolution, which could be compared with the original "Truth DEM". Deviations in the planar surface

within the derived DEM of difference could be then related directly to the parameter which had been modified.

The radial "domes" and the lens model

Initial work in the simulation process focused on confirming the findings of Fryer and Mitchell (1987) in which the systematic error surfaces or "domes" were attributed to an inaccurately estimated lens model. A stereopair configuration was simulated which represents the photogrammetric normal case. This configuration remains important for routine data extraction in photogrammetry, recommended and employed by automated DEM extraction software. The camera base is parallel to the object plane and the optical axes of the cameras intersect the object plane orthogonally. The simulation was employed to calculate photo coordinates for each point of the virtual test field using a known interior orientation and the exterior orientation described before. The parameter k_1, modelling radial lens distortion, was changed to ± 20% before using the GAP software to calculate object coordinates from the computed photo coordinates. The significant alteration of ± 20% for k_1 was chosen, to illustrate the effect of a significantly inaccurate lens model in the object space, and to demonstrate forcibly the capability of the mildly convergent configuration to compensate these effects. The focal length and the parameters for the principal point offset remained unmodified. The computed object coordinates were imported into the ERDAS IMAGINE 8.7 software and a DEM created at 3 mm resolution. Elevation differences from their theoretical values are visualised in Figs. 1 & 2, exhibiting clear evidence of a dome or bowl depending upon the sign of the change. Areas in the DEMs with elevations less than –5 mm are illustrated by solid red colour, whilst solid green regions indicate height differences greater than +5 mm. White areas represent regions of no elevation difference between the "Truth DEM" and DEMs with changing the lens model. Therefore, the deviations in difference DEMs can be related directly to changes in the lens model.

FIG. 1. Elevation differences, k_1 changed by +20% (normal case)

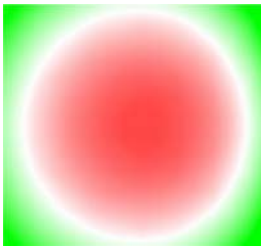

FIG. 2. Elevation differences, k_1 changed by –20% (normal case)

The convergent image configuration

It was hypothesised that a mildly convergent image configuration could perhaps minimise the systematic error surfaces. The exterior orientation of two

photos were derived where the optical camera axes intersect the object plane at the same point, with an angle between these axes of approximately 10 degrees. The parameter k_1 was again changed to +20% which was also used in the normal case configuration (Fig. 1). The simulation process was repeated and a DEM of difference created, illustrated in Fig. 3. It is notable that the "dome" was almost eradicated, particularly evident when taking into account that the DEM representation (Fig. 3) was rescaled to ±1 mm. This is significant as the result indicates potential for mildly convergent image configuration to minimise the residual systematic error surfaces caused by an inaccurate lens model.

FIG. 3. Elevation differences, k_1 changed by +20% (convergent case)

Practical test using a Nikon D80 digital camera

Two Nikon D80 digital cameras (Fig. 4) were purchased for a research project, conducted at Loughborough University to measure flood flows via surface videography and photogrammetry. The need to calibrate these cameras provided the opportunity to validate the findings from the simulation process using real data. A detailed overview of the characteristics of the Nikon D80 camera is given in Table I.

FIG. 4. Nikon D80

TABLE I. Characteristic of the Nikon D80 Camera

Feature	*Nikon D80*
Resolution [pixel]	10 million
Image size [pixel]	3872 × 2592
Size of sensor [mm]	23.6 × 15.8
Size of pixel [μm]	6.095 × 6.095
Auto focus	yes
Manual focus	yes
Dimension [mm]	132 × 103 × 77
Weight [kg]	0.668
Cost [£]	ca. 700

For the calibration process a combined 3D and planar test field was used, consisting of a medium density fibreboard (MDF) (1.2 × 0.9m) to which eight square blocks of various height and shape were added. The interior orientation of

the camera was determined using the self-calibrating bundle adjustment GAP (Chandler and Clarke, 1992). DEMs were extracted; employing the DEM generation tool in the Leica Photogrammetric Suite (LPS) software. The test field, DEM extraction and the calibration process are described in detail in Chandler et al. (2005) and Wackrow et al. (2007). A vertical image pair, representing the normal case, was used for DEM extraction. Two additional images were captured using a mildly convergent configuration with an angle of approximately 8 degrees between the optical camera axes. DEMs were extracted for both configurations. The automatically generated DEMs were compared with the "Truth DEM" which represents the real shape and geometry of the test field. The interior orientation remained unmodified for the DEM extraction process and so changes in elevation differences in DEMs of difference must be related to the change in image configuration. Figs. 5 & 6 illustrate the DEMs of difference for the normal and convergent image configuration in which the elevation differences were scaled to ±3 mm. The radial dome which is apparent in Fig. 5 was virtually eliminated through using the convergent image configuration (Fig. 6) and similar results were achieved using other test images. This result verifies the findings of the simulation process and demonstrates visually the potential of mildly convergent imaging for minimising errors arising from an erroneous lens model.

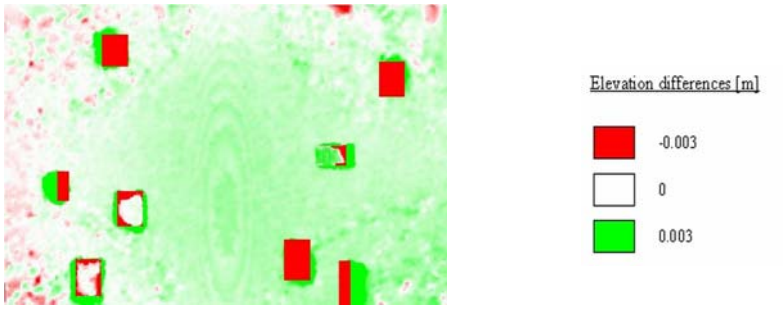

FIG. 5. Elevation differences normal case

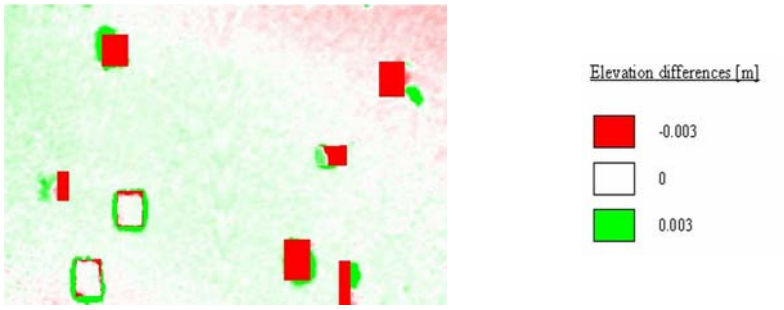

FIG. 6. Elevation differences convergent case

RESULTS

DEM accuracy of the simulation process

Although Figs. 1 & 3 and 5 & 6 provide a convincing qualitative argument, it remains necessary to prove using quantitative data. The accuracy in the object space is best assessed by deriving mean error and standard deviation of error (Li, 1988) from the DEMs of difference. Systematic effects are represented by mean error, whilst the standard deviation quantifies random effects (Chandler et al., 2005). These statistics were generated using an Erdas Graphical Model. Table II summarises DEM accuracy for three tests conducted using the two configurations and simulated data. The first column represents the image configuration used for the simulation, whilst the second column tabulates changes applied to the lens model. The final column represents the mean error and standard deviation of error for the DEMs of difference. As expected, using the normal case and applying changes to the lens model of ±20%, the mean error changed by 1·05 mm and as expected, the algebraic sign switched, whilst the standard deviation of error remained stable. This symmetrical variation is not of concern because mean error and standard deviation of error followed exactly the theoretical expectations.

Using the mildly convergent configuration and a lens model changed by +20%, a mean error of only 0·02 mm and a standard deviation of error of just 0·1 mm for accuracy of DEM generation was achieved. These results are visualised in Figs. 7A & 7B representing cross sections through the DEMs of difference (Figs. 1 & 3) using the normal and convergent configuration. By comparing these DEM accuracy statistics (normal case versus convergent case), it is notable that accuracy using the mildly convergent configuration, increased by 28 times. This simulation is highly significant as it implies that a mildly convergent image configuration can eradicate the systematic error surfaces in DEMs extracted, caused by an inaccurate lens model.

TABLE II. DEM accuracy for the simulation process

configuration/ test	changes in lens model	mean error ± standard deviation [mm]
normal case	+ 20 %	–0·56 ± 2·1
normal case	– 20 %	0·49 ± 1·9
convergent case	+ 20 %	0·02 ± 0·1

DEM accuracy during practical test using the Nikon D80

The presence and the need to calibrate a Nikon D80 digital camera provided the opportunity to validate the findings of the simulation in a practical test. DEMs of difference were created using the normal and convergent case and their mean errors and standard deviations of errors were estimated. These results are summarised in Table III. The first column represents the image configuration used, whilst the second column tabulates mean error and standard deviation of error for the whole of the physical structure of the test field. The camera perhaps achieved poor accuracies using both image configurations but this result was

predicted. Figs. 5 & 6 clearly indicate that overall accuracies were distorted by significant areas of inaccurate data in the vicinity of the wooden blocks due to dead ground or occlusion effects (Chandler et al., 2005; Wackrow et al., 2007). In order to exclude these gross errors from the statistics, mean error and standard deviation of error were also computed for an area of interest situated in the centre of the test object. This represented the flat part of the test field and did not include the wooden blocks. Statistics are tabulated in column two of Table III for both configurations and demonstrate clear accuracy improvement for the mildly convergent configuration. It should be noticed that this specific area is distorted by a dome which is clearly visible in Fig. 5 and also represented by the mean error (0·9 mm) determined for the normal configuration. A mean error of 0·3 mm estimated for the central area of the test object using the convergent configuration identified an increase of accuracy by three times for this region.

To quantify accuracy for the whole imaging area, just data in the vicinity of the wooden blocks were excluded and results summarised in Table III, column four. The accuracy increased by a factor of four, represented by the mean error for the normal (0·4 mm) and convergent configuration (0·1 mm) and visualised also by the cross sections represented in Figs. 8A & 8B.

Again, this result is significant. It demonstrated that the disturbing effect, caused by an inaccurate lens model, was almost eradicated using the mildly convergent configuration and verified the results of the simulation.

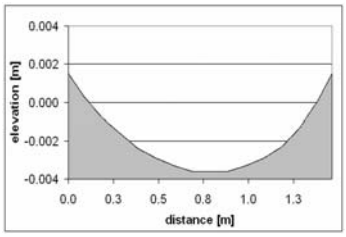

FIG. 7A. Cross section for the normal case (lens model +20%)

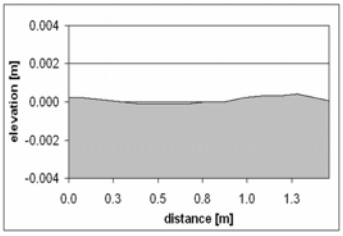

FIG. 7B. Cross section for the convergent case (lens model +20%)

TABLE III. DEM accuracy for the Nikon D80 camera

configuration/ test	full area including wooden blocks (mean error ± standard deviation) [mm]	Central area (mean error ± standard deviation) [mm]	full area excluding wooden blocks/shadow (mean error ± standard deviation) [mm]
normal case	–0·9 ± 9·9	0·9 ± 0·1	0·4 ± 0·4
convergent case	–1·5 ± 10·0	0·3 ± 0·1	0·1 ± 0·2

DISCUSSION

Problems recovering the radial distortion parameters

If accurate camera calibration can be achieved the simulations demonstrated that accurate data can be extracted for all configurations. However, the practical tests using the Nikon D80 digital camera demonstrated the difficulty of recovering perfect lens parameters through self-calibration using the calibration process described in Wackrow et al. (2007). Additional simulation tests were conducted to clarify this difficulty.

A set of interior orientation parameters (focal length, principal point offset and k_1 to model radial lens distortion) was introduced into the simulation and photo coordinates for the *XYZ* coordinates of the test field were estimated using various sets of exterior orientations. These photo coordinates were then re-established into the external self-calibrating bundle adjustment GAP to determine interior and exterior orientation parameters which were treated as unknown. The determinability of these were indicated by comparing the sets of parameters introduced in the simulation and determined by self-calibration.

The configuration (six frames, convergent, two frames rotated) used for camera calibration in Chandler et al. (2005) and Wackrow et al. (2007) was tested initially. The estimated interior orientation parameters were close to their known values but proved inadequate if high accuracy is required. Discrepancies in parameters describing the focal length and principal point offset were not a major concern. These would be compensated by slightly modified exterior orientation parameters because of correlation between interior and exterior orientation parameters, which is well established (Granshaw, 1980; Fraser, 1997; Maas, 1999). However, small discrepancies of the estimated lens distortion parameters relative to their known values remained and consequently degraded the accuracy achievable.

Eleven additional frames were introduced to extend the configuration (convergent, two frames rotated, large horizontal base plus vertical base, two object planes) to possibly increase the determinability of the inner orientation parameters. Only a minor improvement was achieved in determining the exact inner parameters, which could only be justified if fully automated measurement methods are available.

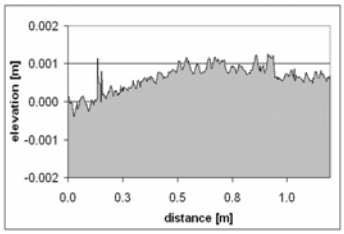

FIG. 8A. Cross section for the normal case

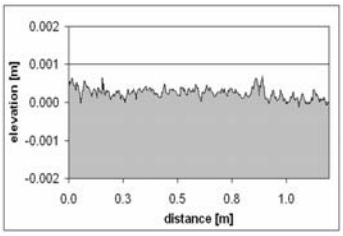

FIG. 8B. Cross section for the convergent case

Finally, a true multi-station camera configuration (perfect configuration) was described by the exterior orientation in which the camera stations were located all around a wholly transparent test field and each control point was visible from each camera station. Although the inner camera parameters were determined perfectly, it has to be recognised that such a configuration is impracticable due to target occlusion.

Summarizing the results, only the perfect camera configuration was capable of recovering the interior orientation parameters completely. The practicable configuration produced acceptable results; certainly for what may be referred as medium accuracy (Fraser, 1997). Unfortunately, the recovered radial distortion parameter differed by 1·5 % from its known theoretical value. This characteristic is a feature of self-calibration that is recognised and has been reported in Honkavaara et al. (2006). The uncertainty involved in deriving completely accurate lens model therefore justifies seeking an alternative approach, which this paper describes. By adopting a mildly convergent image configuration, systematic error surfaces arising from a slightly inaccurate lens model can be eradicated. This suggests that the accuracy of consumer grade digital sensors can be effectively improved, if a mildly convergent configuration is adopted.

Theoretical accuracy of the Nikon D80 camera

The theoretical accuracy in the direction of the camera axis can be expressed using the mathematical term (Luhmann, 2003):

$$s_Z = \frac{h}{b} \times \frac{h}{c} s_{px'} \tag{1}$$

where s_Z is the accuracy in camera direction, b is the length of the photo base, c is the focal length, h is the camera to object distance and $s_{px'}$ is the image precision. The parameter of the stereo image configuration used in this practical test were: b = 0·229 m; c = 0·0245 m; h = 1·6 m and $s_{px'}$ = 0·6 microns. Therefore, the theoretical accuracy or predicted precision in depth for the Nikon D80 digital camera was estimated to 0·27 mm.

In order to evaluate the accuracies of the camera achieved in the practical test, the mean error and standard deviation of DEMs of difference (Table III) can be compared with this theoretical accuracy (0·27mm).

The statistics, estimated for the full test area including the wooden blocks, indicate that the camera performed poorly for both configurations. This result followed expectations as the gross errors, caused by the wooden blocks, disturbed these statistics. It was also not surprising that the camera could not achieve the theoretical accuracy for the central area of the test field using the normal case. This area was effected by a dome, caused by an inaccurate lens model. However, a mean error of 0·3 mm and a standard deviation of 0·1mm estimated for the central test field area using the convergent case indicated that the dome was significantly minimised and the camera almost achieved the theoretical accuracy of 0·27 mm.

The overall accuracy achieved by the camera in this test is demonstrated by the mean error and standard deviation estimated for the whole test object, in which the gross errors caused by the wooden blocks were excluded from the statistics. A mean error and standard deviation of respectively 0·4 mm, estimated using the

normal configuration, demonstrated that the camera performed reasonable well, until this is compared with the value achieved using the convergent configuration, 0·1mm ± 0·2mm. This improvement is highly significant as it demonstrates that the theoretical accuracy of Nikon D80 camera was achieved when the convergent approach was adopted.

Potential impact of findings and future work

The mildly convergent image configuration may be suitable for many spatial measurement applications. Current work is focused on further verifying the findings of this paper by conducting tests using a diverse range of case studies.

Accurate modelling of river bed fabric using digital photogrammetry has been investigated in the past (Chandler et al., 2003) and is still of interest in many scientific and industrial areas. The possibility of assessing a model of a flume river bed, located in a laboratory, provides the opportunity to test the method further in a semi-controlled environment. A non-metric digital camera will be used to acquire a series of images of the flume which describe the normal and convergent configuration. Mosaic DEMs will be extracted and accuracies will be assessed.

Current state of the art computational fluid dynamics (CFD) and in particular, river flow modelling, require accurate estimation of the "free surface" in order to accurately predict the three dimensional flow field along a river. Accurate water surface elevation data are needed to develop computational flow models but it is extremely difficult and dangerous to acquire data during floods. A remote water surface measuring technique could be provided using digital photogrammetry and an additional case study is being conducted to measure a dynamic water surface on a small river, situated in Loughborough. A pair of synchronised digital cameras will be used to capture oblique stereo image pairs (normal and convergent configuration) of the water surfaces. DEMs will be extracted and accuracies will be assessed and analysed.

It is hoped these case studies will demonstrate further that mildly convergent image configuration increases the accuracy of DEMs created using consumer grade digital cameras.

CONCLUSION

The work presented in this paper has successfully identified that using a mildly convergent configuration for DEM generation, minimises the systematic error surfaces caused by slightly inaccurate lens distortion parameters. In addition, a practical test demonstrated that a Nikon D80 digital camera was capable of achieving its theoretical accuracy, if such a configuration was adopted. These results are significant for DEM generation using low-cost digital sensors, where a mildly convergent image configuration can reduce the need for an accurate lens model.

ACKNOWLEDGEMENTS

The authors would like to acknowledge the Engineering and Physical Sciences Research Council (EPSRC) for the first author's studentship.

REFERENCES

CHANDLER, J. H. and CLARK, J. S., 1992. The archival photogrammetric technique: further application and development. *Photogrammetric Record,* 14(80): 241–247.

CHANDLER, J. H., BUFFIN-BÉLANGER, T., RICE, S., REID, I. and GRAHAM, D. J., 2003. The accuracy of a river bed moulding/casting system and the effectiveness of a low-cost digital camera for recording river bed fabric. *Photogrammetric Record,* 18(103): 209–223.

CHANDLER, J. H., FRYER, J. G. and JACK, A., 2005. Metric capabilities of low-cost digital cameras for close range surface measurement. *Photogrammetric Record,* 20(109): 12–26.

FRASER, C. S., 1997. Digital camera self–calibration. *ISPRS Journal of Photogrammetry and Remote Sensing*, 52(4): 149–159.

FRASER, C. S., 2006. Evolution of network orientation procedures. *International Archives of Photogrammetry, Remote Sensing and Spatial Information Sciences*, 36(5): 114–120.

FRYER, J. G. and MITCHELL, H. L., 1987. Radial distortion and close range stereophotogrammetry. *Australian Journal of Geodesy, Photogrammetry and Surveying,* 46/47: 123–138.

FRYER, J. G., CHANDLER, J. H. and COOPER, M. A. R., 1994. On the accuracy of heighting from aerial photographs and maps: implications to process modellers. *Earth Surface Processes and Landforms,* 19(6): 577–583.

FRYER, J. G., 2001. Camera calibration. *Close range photogrammetry and machine vision* (Ed. K.B. Atkinson). Whittles , Caithness. 371 pages: 156–179.

GRANSHAW, S. I, 1980. Bundle adjustment methods in engineering photogrammetry. *Photogrammetric Record*, 10(56): 181–207.

GRENNESS, M. J., OSBORN, J. E. and TYAS, M. J., 2005. Stereo–photogrammetric mapping of tooth replicas incorporating texture. *Photogrammetric Record*, 20(110): 147–161.

GRUEN, A. and BEYER, H. A., 2001. System calibration through self-calibration. *Calibration and Orientation of Cameras in Computer Vision* (Eds. A. Gruen, T.S. Huang). Springer, Heidelberg, 34: 163–193.

HONKAVAARA, E., AHOKAS, E., HYYPPÄ, J., JAAKKOLA, J., KAARTINEN, H., KUITTINEN, R., MARKELIN, L. and NURMINEN, K., 2006. Geometric test field calibration of digital photogrammetric sensors. *ISPRS Journal of Photogrammetry and Remote Sensing*, 60(6): 387–399.

KARARA, H. M. and ABDEL–AZIZ, Y. I., 1974. Accuracy aspects of non–metric imageries. *Photogrammetric Engineering*, 40(9): 1107–1117.

LI, Z., 1988. On the measure of digital terrain model accuracy. *Photogrammetric Record*, 12(72): 873–877.

LUHMANN, T., 2003. Analytische Auswerteverfahren. *Nahbereichsphotogrammetrie – Grundlagen, Methoden und Anwendungen* (2. überarbeitete Auflage). Wichmann, Heidelberg, 586 pages: 233–358.

MAAS, H.–G., 1999. Ein Ansatz zur Selbstkalibrierung von Kameras mit instabiler innerer Orientierung. *Publikationen der Deutschen Gesellschaft für Photogrammetrie und Fernerkundung*, Band 7 (Eds. J. Albertz and S.W. Dech). Weinert, Berlin. 496 pages: 47–53.

REMONDINO, F. and FRASER, C. S., 2006. Digital camera calibration methods: considerations and comparisons. *International Archives of Photogrammetry, Remote Sensing and Spatial Information Sciences*, 36(5): 266–272.

WACKROW, R., CHANDLER, J. H. and BRYAN, P., 2007. Geometric consistency and stability of consumer-grade digital cameras for accurate spatial measurement. *Photogrammetric Record*, 22(118): 121–134.

Zusammenfassung

Die innere Geometrie von digitalen Amateurkammeras wird allgemein als instabil eingeschätzt. Kürzlich durchgeführte Forschungen an der Loughborough University zeigten das Potential dieser Sensoren ihre innere Geometrie beizubehalten. Die Forschungen identifizierten ebenfalls Oberflächen mit systematischen Fehler oder „Kuppeln", sichtbar in digitalen Höhenmodellen (DEMs)(Wackrow et al., 2007), verursacht durch ungenau berechnete Verzeichnungsparameter. Dieser Artikel untersucht die Oberflächen mit systematischen Fehlern und ermittelt eine Methode, diese zu minimieren. Zunächst wurden simulierte Daten verwendet, um den Effekt von Veränderungen der inneren Orientierungsparameter, speziell der Objektverzeichnung, in digitalen Höhenmodelle zu bestimmen. Vorgelegte Ergebnisse zeigen den Zusammenhang zwischen den „Kuppeln" und den ungenau berechneten Verzeichnungsparametern. Das Stereomodell bleibt wichtig in der Photogrammetrie, weil es oft von Software zur automatisierten Erstellung von Höhenmodellen benutzt wird. Der photogrammetrische Stereonormalfall wird oft verwendet, bei welchem die Kamerabasis parallel zur Objectebene ist und die optischen Achsen der Kameras die Objektebene orthogonal schneiden. In der Simulation wurden die Oberflächen mit Fehlern der Höhenmodellen, extrahiert durch Verwendung des Normalfalls, mit den Oberflächen mit Fehlern der Höhenmodelle, erschaffen durch Verwendung eines konvergenten Falls, verglichen. Im Gegensatz zum Normalfall schneiden die optischen Kameraachsen die Objektebene im gleichen Punkt. Ergebnisse des Simulationsprozesses demonstrieren eindeutig, dass eine konvergierte Kamerakonfiguration die Fehler der Oberflächen beseitigt. Dieses Ergebnis wurde durch praktische Tests bestätigt und demonstriert das konvergierte Bilder die Genauigkeit der Höhenmodellen, erstellt mit diesen Sensoren, steigert.